CrystEngComm

RSC Publishing

PAPER

View Article Online
View Journal | View Issue

Dehydration mechanism of a small molecular solid: 5-nitrouracil hydrate†

Cite this: *CrystEngComm*, 2013, **15**, 8202

Maurice O. Okoth,[a] Ranko M. Vrcelj,*[b] David B. Sheen[c] and John N. Sherwood*[c]

Previous studies of the dehydration of 5-nitrouracil (5NU) have resulted in it being classified as a ''channel hydrate'' in which dehydration proceeds principally by the exit of the water molecules along channels in the structure. We have re-examined this proposal and found that in fact there are no continuous channels in the 5NU structure that would contribute to such a mechanism. Product water molecules would be immediately trapped in unlinked voids in the crystal structure and would require some additional mechanism to break loose from the crystal. Through a detailed structural analysis of the macro and micro structure of the 5NU as it dehydrates, we have developed a model for the dehydration process based on the observed development of structural defects in the 5NU crystal and the basic crystallography of the material. The model was tested against standard kinetic measurements and found to present a satisfactory account of kinetic observations, thus defining the mechanism. Overall, the study shows the necessity of complementing standard kinetic studies with a parallel macro and micro examination of the dehydrating material when evaluating the mechanisms of dehydration and decomposition processes.

Received 29th April 2013,
Accepted 6th August 2013

DOI: 10.1039/c3ce40749g

www.rsc.org/crystengcomm

Introduction

It is now well established that the important physico–chemical characteristics of solid phases are dependent upon the crystalline or amorphous form that they hold. It is self-evident therefore that these characteristics will vary if the solid form undergoes a physical change involving a structural rearrangement. There has been a great deal of study of these stability issues with regard to polymorphism.[1] In contrast, there has been much less emphasis on processes relating to the formation and decomposition of hydrated and anhydrous states. Given that much industrial processing is performed in water and that a great number of materials form both hydrated states and associates with water, the role of structure in their inter-conversion is often overlooked. Details of the mechanisms of dehydration/rehydration are determined, in general, from the analysis of kinetic studies on powdered material. Most of this effort has been devoted to the examination of inorganic hydrates. There are few studies into the mechanisms of dehydration of molecular crystals; a topic of increasing interest to the pharmaceutical industry.

Whilst there are a wide range of studies of the kinetics of these processes,[2] it is clear from the large number of mathematical models derived to describe the data,[3] that this is not the most satisfactory method for understanding the underlying processes. To define fully the issues surrounding dehydration (or rehydration), a hierarchical approach must be taken, examining the loss and/or uptake of water at a range of levels, from the molecular, through to the full single crystal. Only in this way can a true understanding be made of the process and how it can relate to the kinetic data.

A previous paper from the authors has shown how the mechanism of water loss from oxalic acid,[4] a simple molecular dihydrate, can be understood by structural considerations and how these relate to the resulting kinetic studies. This understanding of the dehydration mechanism is informed by important work by Galwey, with his WET classification of metal–organic hydrates, the structural/energetic classifications of Petit and Coquerel and the early work of Perrier and Byrn on hydrate channels existing in crystals.[5] These classifications are all discussed in detail in the previous paper.

As part of a programme to study dehydration/rehydration phenomena, we have examined a number of molecular materials with differing structural motifs. One of these materials is 5 nitrouracil (5NU) $C_4H_3N_3O_4$ a cyclic urea derivative with a strongly electron accepting nitro-group. It also possesses notable N–H bonds and C=O groups, with the potential of forming strong intermolecular H-bond interactions (Fig. 1). 5NU exhibits not only hydrated structures but also polymorphism; two hydrates and three anhydrous polymorphs have been identified to date. Only two of the

[a]*Department of Chemistry & Biochemistry, Chepkoilel University College, Moi University, P. O. Box 1125-30100, Eldoret, Kenya*
[b]*Chemistry, Faculty of Natural and Environmental Sciences, University of Southampton, Highfield Campus, Southampton, SO17 1BJ, UK.*
E-mail: r.vrcelj@soton.ac.uk; Fax: +44 (0)2380 596723; Tel: +44 (0)2380 596722
[c]*WESTCHEM, Department of Pure and Applied Chemistry University of Strathclyde, Thomas Graham Building, 295 Cathedral Street, Glasgow, G1 1XL, UK*
† Electronic supplementary information (ESI) available. See DOI: 10.1039/c3ce40749g

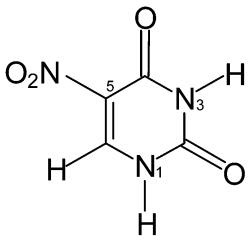

Fig. 1 Structure of a 5-nitrouracil molecule.

anhydrous forms (centrosymmetric orthorhombic and monoclinic forms) and one hydrated form can be obtained by crystallisation from pure water.[6] A third anhydrous polymorph (non-centrosymmetric orthorhombic) is only generated from organic solvents[6] and the second hydrated form is a result of crystal engineering experiments by Pereira Silva *et al.*,[6] who added L-lyseine to the solution to direct the crystallisation. In crystallisation from aqueous solution, 5NU shows an Ostwald like staged behavior, in that the anhydrous forms crystallise first (which form crystallises depends upon temperature), followed by the final nucleation and growth of 5-nitrouracil monohydrate from the suspended anhydrates by a solvent mediated transformation.[7]

In the only previous work on the dehydration of 5NU, Perrier and Byrn[5] noted that 5NU dehydrates by a randomly dispersed nucleation process. Inspection of the crystal structure led them to note the existence of molecular channels by way of which the product water molecules could leave the crystal and proposed that this was a key factor in the dehydration mechanism. Much work still remains to be done to define the detailed mechanism of dehydration of this material and its relationship with the measured kinetics of the process. In this paper we extend the work that has been performed on oxalic acid to 5NU, to examine the thermal dehydration of 5NU and so to elucidate the mechanism and better understand the kinetics of the dehydration process. A simultaneous study of the structure of the hydrate provides clues to the role it plays in water loss during dehydration.

Experimental

Preparation of samples

5-Nitrouracil monohydrate (Sigma Chemical Co. Poole, UK 99% purity), was re-crystallised from double distilled water at 25 °C and crystalline plates of the hydrate (length ~2–6 mm) were harvested after 96 hours at 25 °C. To obtain different size fractions, dried material was gently pulverized with a pestle in a mortar and then sieved through mesh sizes (425, 125 and 100). The size fractions of 425 μm–125 μm, 125 μm–100 μm, and <100 μm are referred to as 425 μm, 125 μm and 100 μm. All samples were stored over a saturated solution of calcium sulphate to prevent dehydration of 5NU, which occurs readily when the hydrate is exposed to ambient relative humidities.

Differential scanning calorimetry (DSC)

Data was collected on a DSC V2.2A Du Pont 9900 DSC. Sample weights of 6–10 mg were used. Samples were run at a scanning rate of 10 °C min^{-1} using nitrogen as a carrier.

Thermogravimetric analysis (TGA)

Non-isothermal thermogravimetry was performed using a Seiko Denshi Kogyo TG/DTA 200 instrument. The samples were heated in open sample pans (sample weight 5 mg) under dry nitrogen at a heating rate of 10 °C min^{-1}.

X-ray powder diffraction (XRPD)

Room temperature, XRPD, was performed at the University of Southampton, on a Bruker C2 diffractometer, utilising Cu Kα radiation.

Atomic force microscopy (AFM)

These were conducted with a Quesant Resolver 250 AFM, using Si_3N_4 integral tips with a spring constant of 0.22 N m^{-1} in conjunction with a scan head with a maximum range of 14.6 × 14.6 μm for both micron scale and high resolution imaging. The scanner was calibrated with Highly Oriented Pyrolytic Graphite and muscovite mica.

Scanning electron microscopy (SEM)

Scanning electron micrographs were taken on a JEOL JSM-35 scanning electron microscope.

Thermomicroscopy

A Reichert Polyvar 2 microscope was used for transmitted light microscopy, and for thermomicroscopy, a Mettler FP 5 and a FP 52 system was used.

Thermogravimetry

For isothermal studies, a CI Robal electronic micro-force balance was used. Data was collected electronically using an in-house designed AD converter. Control of relative humidity (RH) was achieved by passing dry nitrogen gas through a set of saturated solutions; KOH (8% RH), $CaCl_2$ (30% RH), KBr (58% RH), NaCl (75% RH), KCl (84% RH). Temperature control was achieved using an in-house designed bath surround.

Sample control

For comparative studies it is important to keep sample weights constant. Agbada[8] has shown that an inverse relationship that exists between the sample weight and the activation energy is attributable to the greater self-cooling effect of a larger sample mass on endothermic reactions.

Nomenclature

For brevity, we refer to the crystalline forms of 5NU as; 5NU-h for the monohydrate form, 5NU-o for the anhydrous centrosymmetric orthorhombic form and 5NU-m for the anhydrous centrosymmetric monoclinic form. Two other crystalline forms of 5NU (anhydrous non-centrosymmetric and the hydrate of Pereira Silva) were not seen in this study.

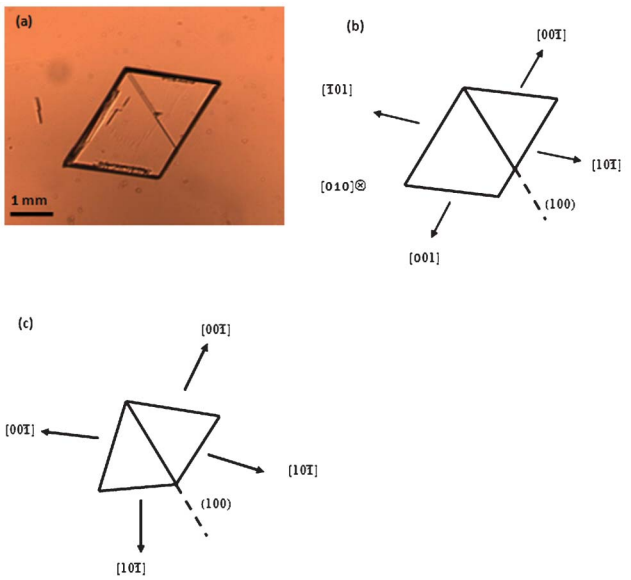

Fig. 2 (a) Untwinned 5NU-h crystals; (b) morphology and (c) schematic of a twinned crystal.

Results and discussion

Crystal growth and morphology

A detailed description of the crystal growth of 5NU from aqueous solutions, the effects of polymorphism and the role of twinning has been given by Okoth *et al.*[7] In the present studies; crystals of 5NU-h were thin, rhombohedral tablets (Fig. 2), with a main face of (010). The bounding facets are; $(\bar{1}01)$, $(10\bar{1})$, $(00\bar{1})$ and (001), often with {100} facets showing or well developed. Fig. 2a shows the line of [100], in this case simply as a line defect in the crystal, however, it also acts as a twin, a simple 180° rotation around [100]: and a schematic of a constructed twinned crystal is given in Fig. 2c. Twinned crystals of this type are the most commonly seen, however as previously reported, a number of other twins also exist for 5NU-h. The indexing of the faces used in this study is derived from the recent crystallographic determination by Okoth *et al.*[7]

Dehydration product

The dehydration product was shown by XRPD to be 5NU-o. The unit cell parameters for 5NU-h and 5NU-o are given in Table 1.

Table 1 Crystallographic data for 5NU

	5NU-h	5NU-o
CCDC ref. code/deposition no.	871417	NIMFOE01
a (Å)	5.0642	8.308
b (Å)	21.9255	10.426
c (Å)	6.1176	13.363
β (°)	113.1	90
Space group	$P2_1/c$	*Pbca*
Volume (Å^3)	624.8	1157.5
	4	8

Structural assessment

The crystal structure of 5NU-h (Fig. 3) shows a layered structure, with both 5NU and water molecules lying in the $(10\bar{2})$ plane (Fig. 3a). Within the plane, there is hydrogen bonding between the 5NU and water molecules, with the hydrogen atoms of the water molecule yielding bifurcated h-bonds. These planes of molecules are separated by ~2.979 Å and are bonded by van der Waals forces. Viewed along the *a*-axis (Fig. 3b), it appears that there is an easy route for water to leave the structure which corresponds to the linked voids identified by Perrier and Byrn, who calculated the void cross-sectional area to be small, 1.84 Å^2. Closer examination shows however that these apparent channels do not exist and the structure is an isolated site hydrate (Fig. 4). Examination of the van der Waals radii shows that the largest available cross-sectional area that is available is <0.5 Å^2 which is too small for a water molecule to pass through (where the smallest dimension of a water molecule is ~2.4 Å).[9] The potential for an easy passage of the water to any surface therefore does not exist.

The earlier work of Okoth *et al.*[7] has shown that there exists a limited structural relationship between 5NU-h and 5NU-o, which simply consists of a localized molecule–molecule motif; a loose dimer, with no extended supramolecular structure or long-range ordering. This local interaction is shown in Fig. 5 and is similar for 5NU-h and 5NU-o. The main difference between the structures is the extended network of hydrogen bonding outside this dimer pair. For the hydrate structure, this extends in sheets incorporating the next molecules, which are water molecules, whereas for 5NU-o and 5NU-m, these have weaker bondings, out of the plane of the dimer molecules and clearly connecting to other 5NU molecules. The structural relationship between the hydrate and the product is thus at the best a weak one. It would not facilitate an easy transition from the hydrated structure to the anhydrous crystalline form.

Dehydration studies

Reflection optical microscopy. Fig. 6a shows a schematic of the main visible features, and 6b shows the surface of a fresh 5NU-h crystal. In addition to the crystal facets described above, there can be seen the [100] twinning plane and growth striations spreading from this and running parallel to $(10\bar{2})$. Higher magnification (Fig. 6c) shows the growth features in finer detail and confirms that between the growth striations the surface is generally smooth. After 2 hours at 40 °C (Fig. 6d), there is a general contrast enhancement at the growth striation boundaries. This is typical of defective volumes during dehydration. These striations are effectively acting as major fissures on the (010) surface, from which the hydrate water can escape more easily. The disordered product remains isolated in the defect leading to the observed contrast enhancement. The higher resolution image (Fig. 6e) details the above, and also reveals a formation of oval "mottled" markings at the (010) surface, with the long axis of the oval lying parallel to $(10\bar{2})$. Also seen is the initiation of fine cracks of the same general orientation. The mottling indicates sites where water lost from the surface of the crystal (in relatively perfect areas) initially accumulates before subsequent evapora-

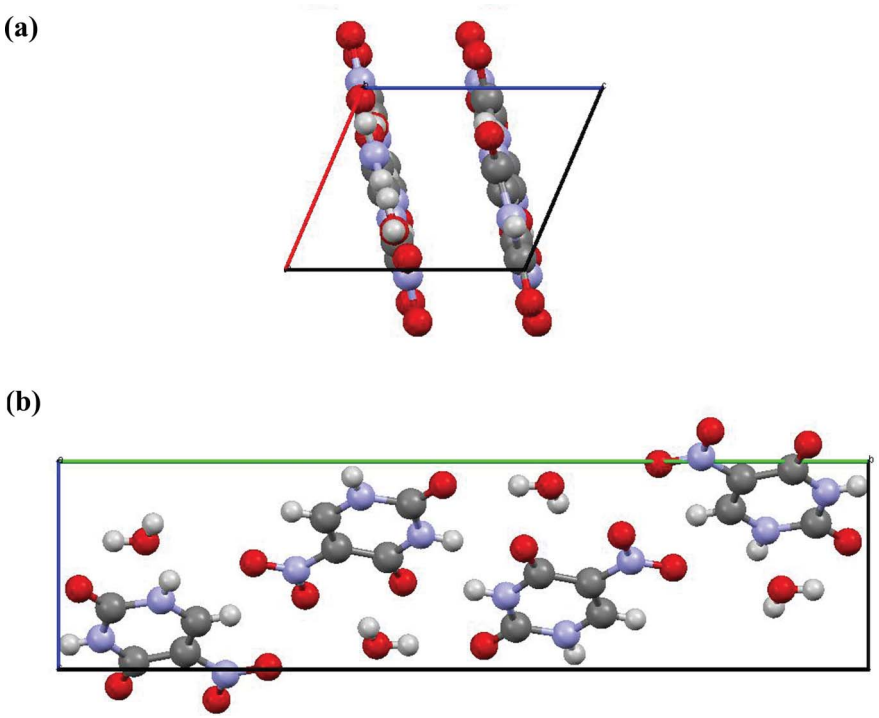

Fig. 3 (a) Viewed along the *b*-axis, showing the layered structure of 5NU hydrate and (b) viewed along the *a*-axis, showing the possible channels along which the waters lie.

tion. This assumption was confirmed by the observation of water condensation at these sites. As such, the dehydration process appears to consist of two competing processes, loss of water from major defective areas (*e.g.* growth striation boundaries) and that from the developing micro-cracks where they emerge at the surface. As dehydration proceeds (Fig. 6f), the change in contrast of the growth striations does not measurably increase, but more micro-cracks develop. (Fig. 6g). Higher magnification also shows further mottling. The number of new cracks and the degree of mottling increases with time, rather than each growing to much larger sizes. The cracks must result from the increased partial pressures of the water vapour under the surface layers within the crystal, and provide the major routes for water to escape.[10]

Transmission optical microscopy. Fig. 7 shows a set of typical transmission optical micrographs of a 5NU-h crystal at 40 °C. A schematic is given in Fig. 7a. The fully hydrated crystal is shown in Fig. 7b, with the unit cell axes given as a reference and the well-formed faces being $(10\bar{1})$. Within the crystal, there are sets of lines visible that are parallel to [100] and also some fainter lines that start from the central line that is associated with [100] and are set at an angle of $\sim 67^{\circ}$, showing that they are parallel to $(10\bar{2})$. The central, most well contrasted line, is the regularly observed major twin boundary separating the two twinned parts of the crystal. The fainter lines parallel with this are likely to be localized, mechanically induced, twinned

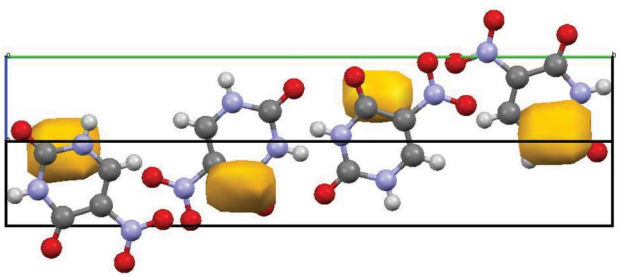

Fig. 4 Calculated voids in the 5NU-h unit cell.

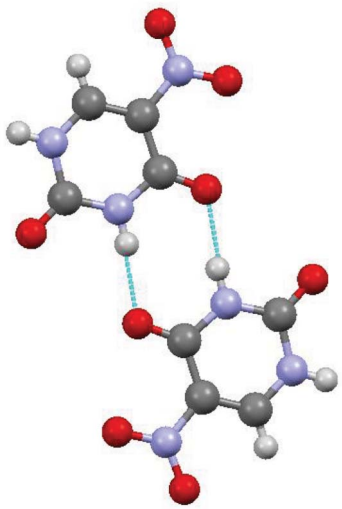

Fig. 5 Weak dimeric structure common to 5NU-h, 5NU-o and 5NU-m.

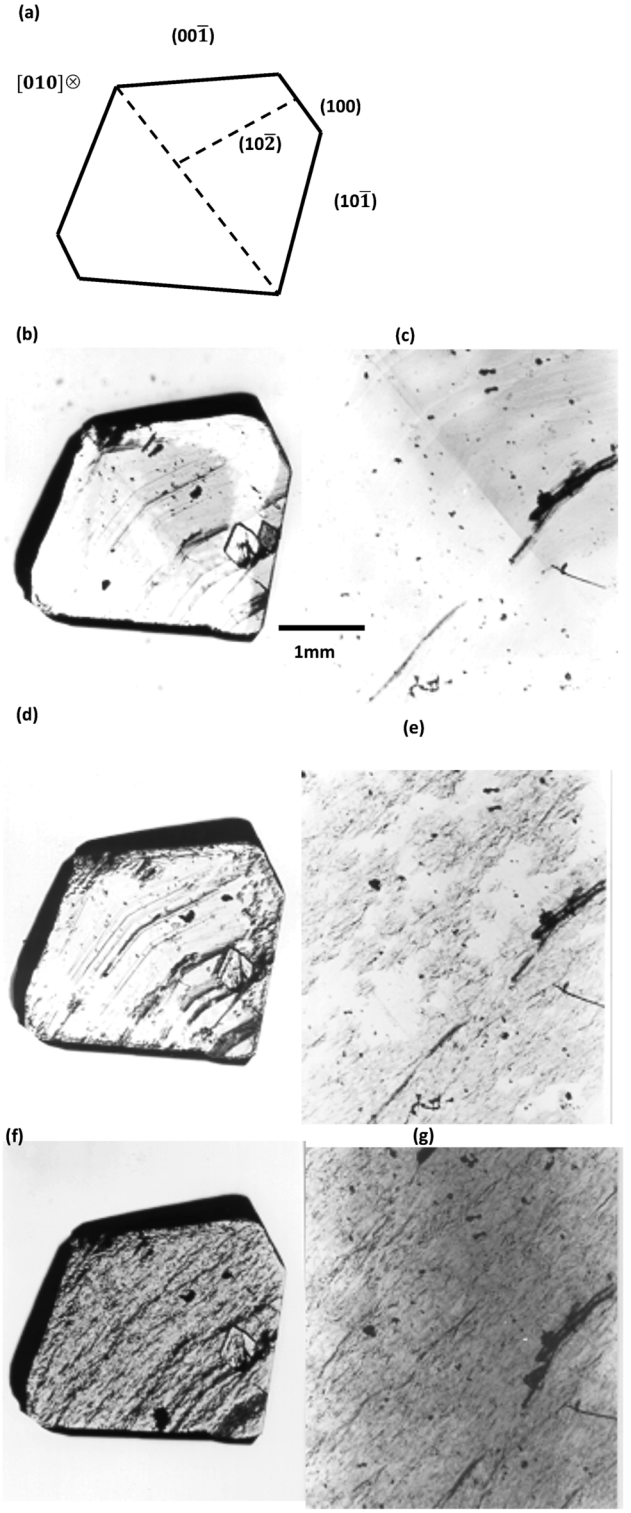

Fig. 6 The (010) surface of 5NU-h at 35 °C at magnifications ×25 and ×100. (a) Schematic of the crystal at ×25, indicating the main faces visible (00$\bar{1}$), (100), (10$\bar{1}$), and indicating the trace of visible features (dashed lines) associated with (100) and (10$\bar{2}$) Miller indices. (b) and (c) 0 hours; (d) and (e) 2 hours; (f) and (g) 5 hours.

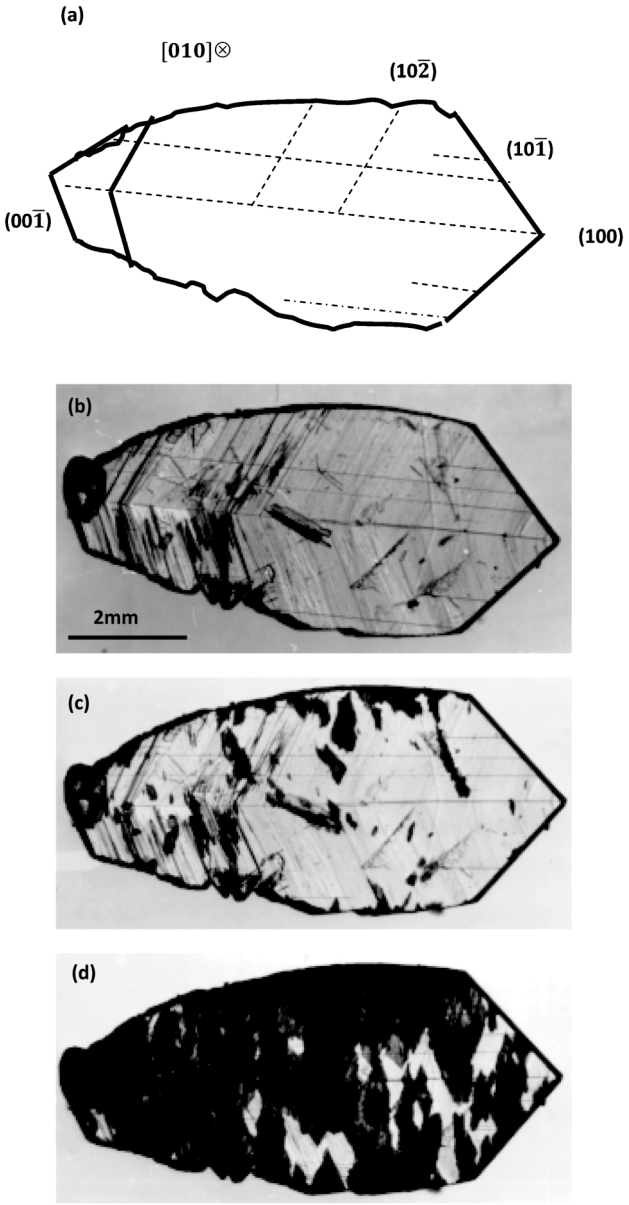

Fig. 7 Transmission optical micrographs of the dehydration of the (010) face of 5NU-h; (a) schematic, indicating the Miller indices of the observable planes or feature, as labeled in Fig. 6a; (b) 0 hours; (c) 1.5 hours; (d) 3.0 hours.

defects. This interpretation is consistent with the observation that most of these appear to have been initiated at the small inclusions that lie at their ends and from which they propagate towards the bounding facet. The multitude of striations parallel to (10$\bar{2}$) are growth striations developed during the growth of the crystal. During the dehydration process neither of these defects show any significant changes and thus they play no part in the decomposition process.

As the crystal dehydrates (Fig. 7c), opaque zones begin to emerge, primarily at the edges of the crystal – these are associated with water loss and the reduction in the transparency afforded by the change from single crystal to a powder. As the dehydration progresses (Fig. 7d), the opacity of the crystal

increases, but it is of note that the opaque areas have a fan-like image. The angular spread subtended by these fans is $\sim 40^{\circ}$, equivalent to that between [001] and $(10\bar{2})$. The dehydration is complete after 4.5 hours.

Scanning electron microscopy. Scanning electron micrographs of 5NU-h and 5NU-o are shown in Fig. 8. The high vacuum in the instrument causes immediate dehydration from the surface of the hydrate and this water loss appears as striations across the (010) surface, (Fig. 8a). These microscopic striations subtend the same angle to the edge of the crystal as do the growth striations seen in the optical microscopy and hence, lie along the emergent $(10\bar{2})$ planes. The fully dehydrated surface is seen in Fig. 8b. There is little obvious structure, although it is possible to see older striations (as seen in Fig. 8a) underneath the recrystallized surface layers. It is noteworthy that similar patterns are visible on an adjacent lateral facet (positioned at the right hand edge of the crystal) in Fig. 7b confirming a general involvement in reactivity of the $(10\bar{2})$ plane.

Atomic force microscopy. High resolution atomic force microscopic studies of the (010) surface of 5NU-h crystals show a relatively smooth surface (Fig. 9a), with gentle undulations across the surface and low variation in the general height of the surface (<35 nm). There exist a few isolated regions that show a greater variation in height, but these larger differences can be ascribed to contaminating particles adhering to the surface. After dehydration (Fig. 9b), there is a much greater variation in the surface heights, of an order of magnitude, and as with optical microscopy, cracks can be seen on the surface. It is of interest that the grosser changes seen in optical and electron microscopy are not seen in the AFM images. This is most likely due to the limited area that can be observed using this technique. So the cracks and striations are truly macroscopic in nature, rather than many smaller cracks and some larger ones being more visible in microscopy.

Thermal studies. Isochronal TGA shows a total weight loss of 10.3%, consistent with the expected calculated value. This mass loss occurs between 70 °C and 100 °C, consistent with the observed dehydration endotherm observed using DSC. No further mass loss occurs until the 5NU commences decomposition just before 300 °C, although there is phase transformation between the dehydrated 5NU-o and 5NU-m at $\sim$260 °C, as noted in the earlier publication of Okoth *et al.*[7]

Dehydration at the molecular level. Key to an explanation at this level is the evidence from the general structural part of this study of the role of the $(10\bar{2})$ planes in the dehydration process. They appear to be the principal route by which water eventually leaves the structure but at the same time show no obvious and easy direct route from the interior of the crystal to the surface. A consideration of the planar nature of the 5NU-h molecule and its presence in sheets of hydrated planar molecules lying in adjacent $(10\bar{2})$ planes leads to a relatively straightforward understanding of the loss of water at the molecular level. Within the plane of the molecules, the waters are surrounded by four 5NU molecules and strongly bound within the plane. The planes of molecules intersect the main (010) face (Fig. 10). Thus, there will be water molecules that are exposed and partially bonded to the molecules beneath them.

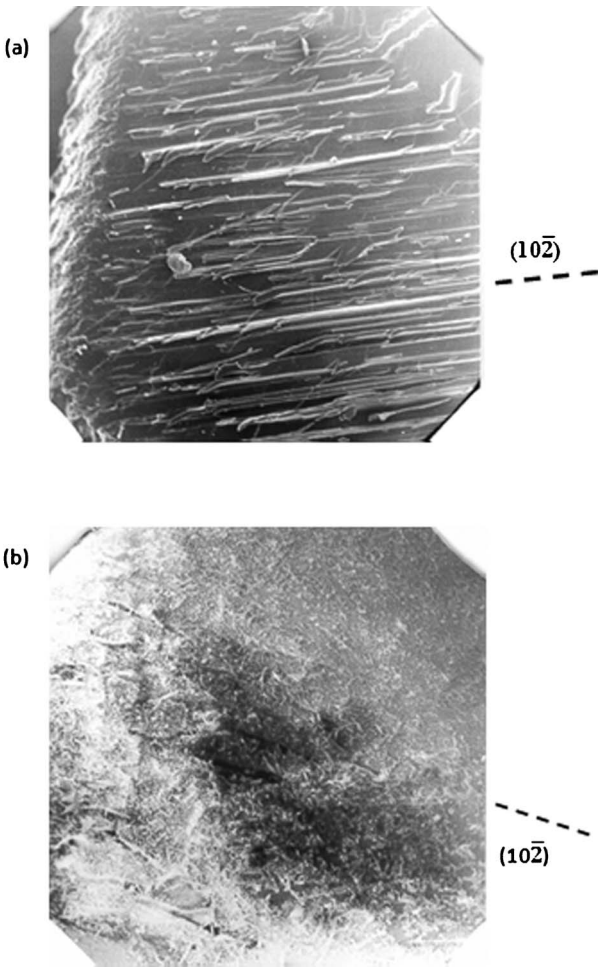

Fig. 8 Scanning electron micrographs showing the surface of the (010) faces of (a) hydrate and (b) dehydrated samples (magnification ×40). The $(10\bar{2})$ planes are indicated.

These will be the first molecules to leave the crystal. As they do so, this permits a reorganization of the surrounding 5NU molecules and this will be centred on the common dimer motif described earlier. As there are no strong bonds between the planes of molecules, only van der Waals forces, the remaining 5NU molecules are relatively free to generally disassociate from the structure. This will lead to a self-reorganization close to the surface and also a further weakening of the interplanar bonds, permitting more water to escape along that particular direction and for cracks to start forming. This explains the mottling seen in Fig. 5 and the cracking running parallel to the direction of the planes of molecules, as seen emerging at the (010) surface. A reorganization of this sort will eventually lead to a proper recrystallisation of the product phase. Since there is very limited long range similarity between 5NU-h and 5NU-o then, as the recrystallisation occurs, this will block off the exit routes for the water.

As dehydration proceeds, there is likely to be even more disorder within the dehydrating areas. So as the dehydration and recrystallisation occurs, this blocking of the exit routes

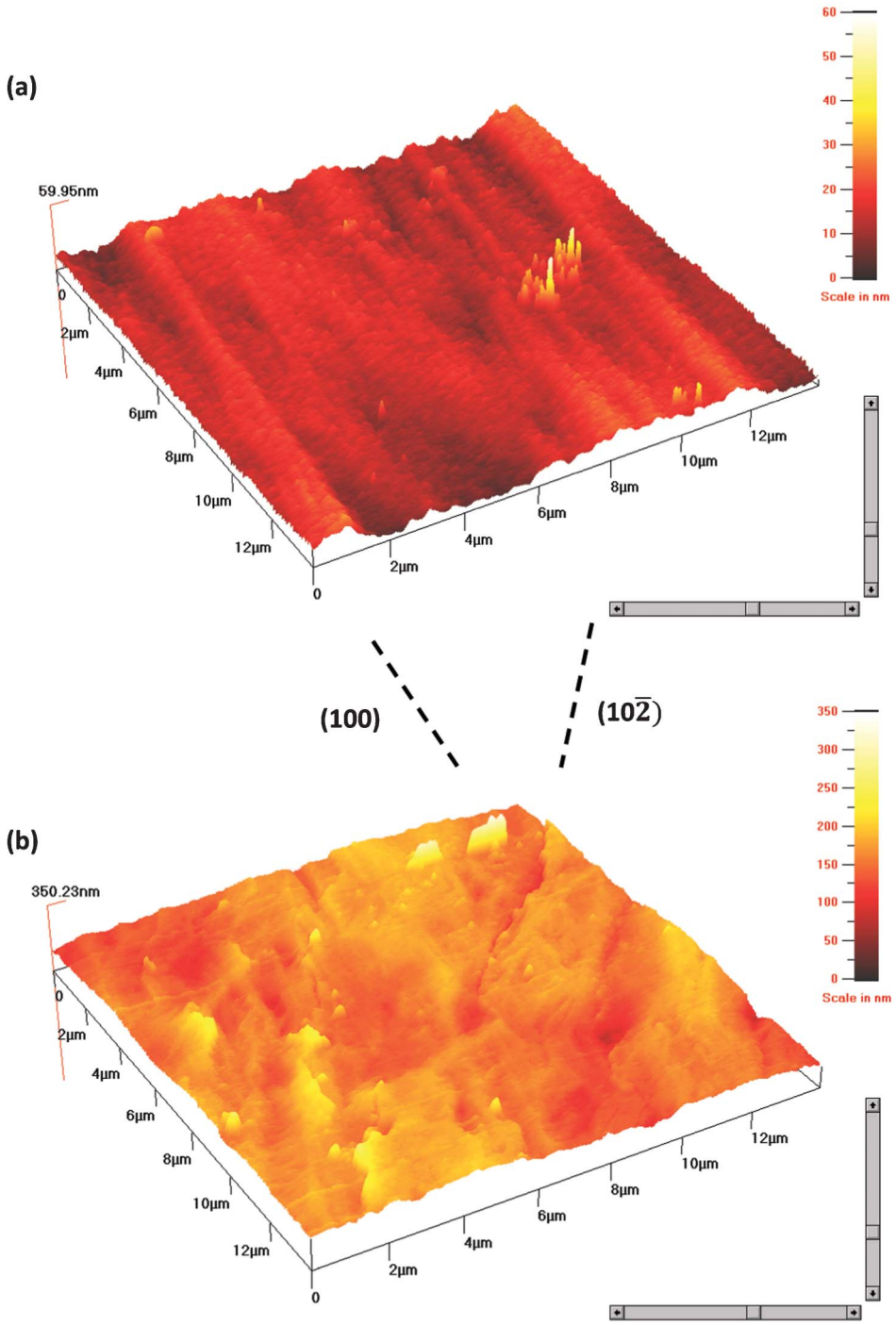

Fig. 9 AFM scan of the (010) crystal surface of (a) 5NU·H_2O and (b) anhydrous 5NU dehydrated at 35 °C. (100) planes are indicated as are the (10$\bar{2}$) planes.

will cause the remaining (underneath this surface) 5NU-h to stop losing water at the initial rate. However, when the vapour pressure of the water is great enough, it will break through the intermediate layer of recrystallised material at weak points and the dehydration will recommence. This would imply that the dehydration process is stepwise, with weight loss occurring in discrete periods of time, all due to a lack of structural coherence between parent and product.

Kinetic studies

Typical isothermal fractional dehydration (α–t) curves are shown in Fig. 11. These show an overall sigmoidal dehydration processes, but this is interspersed with periods when no water is lost from the material. This type of stepwise behaviour is predicted from the structural analyses given earlier in this paper and has previously been noted during the dehydration of oxalic acid. In the case of oxalic acid, the periods of no water

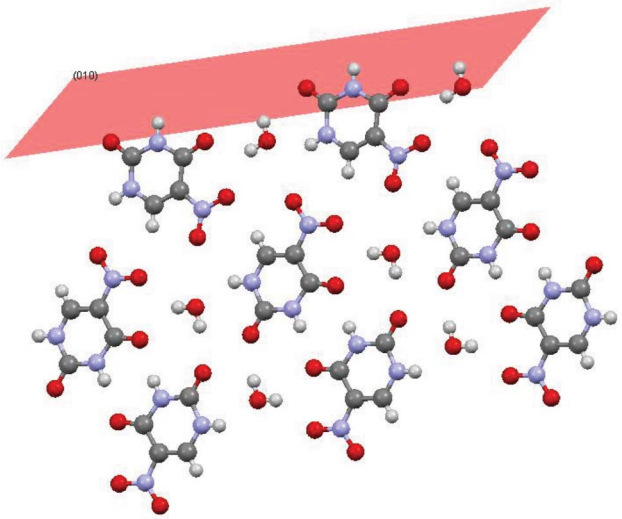

Fig. 10 Molecular packing of 5NU-h near the (010) surface.

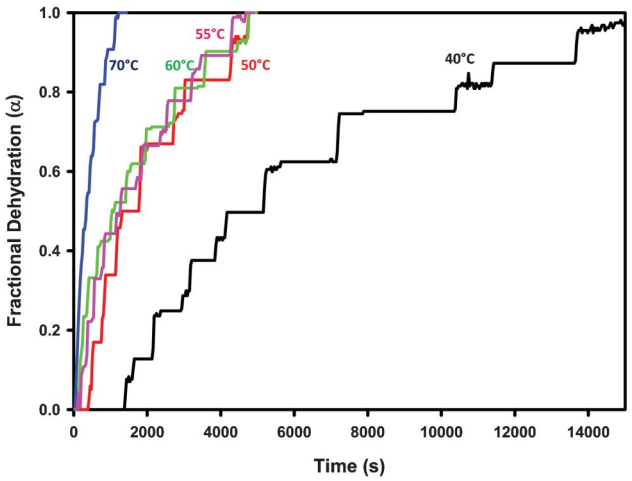

Fig. 11 Thermal dehydration of 5NU-h – the temperature of each dehydration is indicated by the colour of the run and the temperature label on the figure.

loss were shorter and less water was lost between each period of stasis, giving a closer approximation to a monotonically increasing curve. It was shown in this case that the pauses in water release could be exaggerated by coating the oxalic acid in an impermeable layer.

This behaviour immediately raises the issue of how should the data be analysed? There are two clear options. Firstly, to simply analyse the data as is – effectively taking an average of the data. The second option is to treat each isolated loss of water as a separate event. Both approaches have a major limitation, in that neither method really takes into account what is occurring at the molecular and other hierarchical levels. In particular, whether the data is treated as a whole or split up into several discrete sections of dehydration, the kinetic models only examine the possibility of disassociation of water and a generalized transformation into an anhydrous phase. How the water physically leaves the system (in the case of 5NU, *via* cracking of the crystal and more limited surface dehydration effects) is not considered, as has been discussed previously by Galwey and Petit and Coquerel.[5]

Although it may be possible to observe changes in the kinetic models by splitting the data into separate sections, the mass loss events are small in quantity and short in time, making accurate measurements problematic. For this reason we have chosen to use the ''average'' method of curve fitting. This may be more useful in an overall viewpoint of the process, permitting comparison between each set of experiments and at least an idea of the timescale of the dehydration process. However in doing this, care need be taken when citing values for thermal and materials parameters.

Effect of temperature. Fig. 11 shows typical dehydration curves at a range of temperatures (40–70 °C). Used for this particular determination were 'as crystallised' single crystals with dimensions of approx. 1 mm. Each curve increases monotonically only in an approximate manner. As the temperature increases, the rate of water loss also increases, but even at relatively high temperatures, there are still periods when the water loss stalls, more noticeable at higher amounts of water loss. Also of note is the fact that although the rate of water loss increases, it does not do so gradually. Water loss at 40 °C is slow, and at 70 °C is much faster. But in the range of 50–60 °C, the water loss curves are effectively the same (an additional curve run at 55 °C is shown in Fig. 11 to emphasise this fact). This may well be related to the two different mechanisms of water loss. At lower temperatures, one of either cracking or defect generation is dominant, at higher temperatures, the other is dominant. At intermediate temperatures, neither one is.

Attempts to fit known curves of dehydration to the data presents further issues (in addition to those discussed earlier). Of the very wide range of mathematical mechanistic models (circa 20) that have been proposed as potential ''fits'' for decomposition kinetics, two fit the present data well. These are (i) the one-dimensional diffusion relationship (parabolic law, $D_1(\alpha)$) and (ii) the two-dimensional diffusion relationship (Valensi–Barrer, $D_2(\alpha)$);

$$\text{Parabolic law, } D_1(\alpha)\text{:Valensi}-\text{Barrer equation. } D_2(\alpha)\text{:}$$

$$\alpha^2 = kt\text{:}(1-\alpha)\ln(1-\alpha)+\alpha = kt$$

Table 2 shows the similarity of these two best fitting models. It is clear that from a purely mathematical perspective, these two models are indistinguishable. From a mechanistic perspective, we may assume that the physically derived Valensi–Barrer equation would be the preferred model as it describes a two-dimensional cylindrical diffusion event. Clearly from our examination of the structure of 5NU-h, this is not anywhere close to the real case. Issues like these re-emphasise the fact that although these kinetic models can often fit observed data well and subsequent thermal characteristics can be calculated from them, they do not necessarily describe truly the ongoing process. From a practical point of view, it is possible to develop an Arrhenius

Table 2 Best fitting kinetic models for isothermal dehydration

Temperature (°C)	Best-fitting mechanism	Second best-fitting mechanism
40	$D_1(\alpha)$ (0.977)	$D_2(\alpha)$ (0.962)
45	$D_2(\alpha)$ (0.977)	$D_1(\alpha)$ (0.973)
50	$D_2(\alpha)$ (0.968)	$D_1(\alpha)$ (0.960)
55	$D_1(\alpha)$ (0.987)	$D_2(\alpha)$ (0.959)
60	$D_2(\alpha)$ (0.978)	$D_1(\alpha)$ (0.978)
65	$D_2(\alpha)$ (0.990)	$D_1(\alpha)$ (0.951)
70	$D_1(\alpha)$ (0.987)	$D_2(\alpha)$ (0.976)

plot using data from both kinetic models (Fig. 12). It is of interest that even using two appreciably different kinetic models, the thermal parameters so derived are identical. In the case of the parabolic law ($D_1(\alpha)$), an activation energy of 76(5) kJ mol^{-1}, and frequency factor of 3.67 × 10^8 s^{-1}. For the Valensi –Barrer model ($D_2(\alpha)$), the activation energy is 78(6) kJ mol^{-1} and a frequency factor of 7.61 × 10^8 s^{-1}. These activation energies can be compared to that derived by the non-isothermal Ozawa method[11] based on the TG data with a change in the heating rate, and found to be 76.5 kJ mol^{-1}. Within limits of experimental errors, the values obtained from the two methods are identical.

The slowing down of the dehydration at higher dehydrated fractions is a combination of both the general deceleration of the process, but is also dependent upon the mechanism of water loss. In the early stages of water loss, it is relatively easy for water to force a path out of the crystal. However, once phase reorganization occurs and blocks the existing pathway, these either have to be cleared or new pathways found for the water to leave the crystal. The more dehydration occurs, the more complex and difficult the pathway is for water egress. So even at high temperatures (*e.g.* at 70 °C), there are still periods when water cannot leave the crystal.

Effect of particle size and relative humidity. One immediate effect of grinding 5NU-h is that it causes a decrease in the amount of water within the samples. Water is liberated during the grinding process and so much is freed, that in attempting to sieve and size fraction samples for experiments, it was impossible to generate small (<20 μm) sample sizes with only a slurry resulting. Although the bulk of the sample remained as 5NU-h, no other crystalline form was observed; hence we attribute this to partial amorphisation of 5NU during the grinding process. This loss of water is shown in Table 3.

Table 3 Decrease of water content with reduction in particle size

Particle size range	% Water content
125–425 μm	10.1 ± 0.1
100–125 μm	9.9 ± 0.5
<100 μm	9.3 ± 0.5

Typical α–time plots for the three different particle sizes are shown in Fig. 13. As would be expected, the smaller the particle size, the more rapid the dehydration. It is also noticeable that the stepwise manner of the dehydration still occurs for all these particle sizes. At smaller particle sizes the stepwise dehydration is less pronounced, but still extant. Similarly to the case of the as-crystallised materials, the longest periods of quiescence occur later in the dehydration process.

As with the simple thermal studies described earlier, fitting kinetic models to these curves is not straightforward. As well as the two diffusion based models described earlier, a variety of other models also fit the data well. These range from diffusion based models, phase boundary models and nucleation models. The frequency with which they are best fits to the data is given in Table 4. Structural intuition would let us say that indeed the dehydration is some form of mix of a diffusion process, with phase boundary events occurring as well as other nucleation processes. Although the best fitting models were varied, the Valensi–Barrer model was always either the best or second best fit, so for deriving thermal parameters, we continue to use this model as a means for generating numerical values.

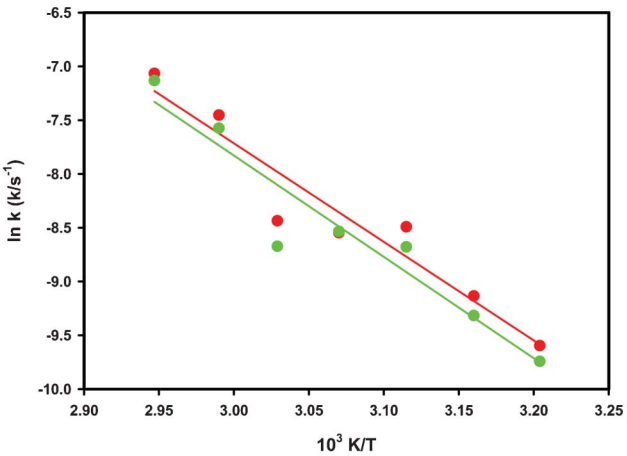

Fig. 12 Arrhenius plots for the thermal dehydration shown in Fig. 11. Green is the $D_2(\alpha)$ model and red the $D_1(\alpha)$ model.

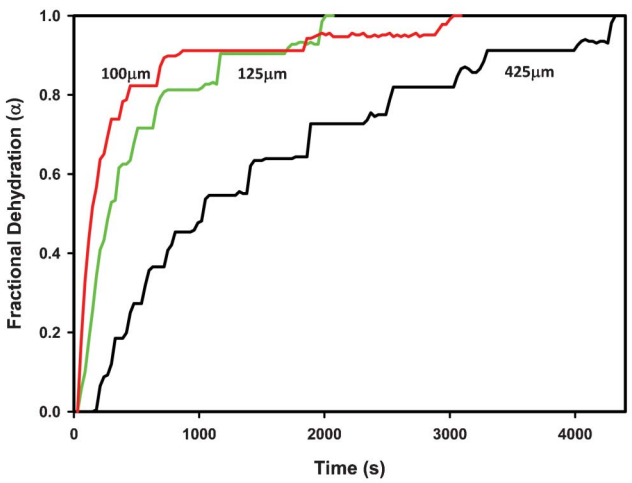

Fig. 13 Thermal dehydration of 5NU-h, with differing particle size.

Table 4 Comparison of the frequency of best fitting kinetic models for the dehydration of different particle sizes of 5NU-h at 0% RH[a]

425 μm		125 μm		100 μm	
Model	Frequency (8 runs)	Model	Frequency (6 runs)	Model	Frequency (8 runs)
$D_2(\alpha)$	3	$D_2(\alpha)$	3	$D_2(\alpha)$	4
$D_4(\alpha)$	2	$D_4(\alpha)$	1	$D_1(\alpha)$	2
$D_1(\alpha)$	2	$A_1(\alpha)$	1	$A_2(\alpha)$	1
$R_2(\alpha)$	1	$A_3(\alpha)$	1	$A_3(\alpha)$	1

[a] Key to kinetic models:[12] $D_1(\alpha)$ – Parabolic law, $D_2(\alpha)$ – Valensi–Barrer, $D_4(\alpha)$ – Ginstling–Brounshtein, $R_2(\alpha)$ – 2-D phase boundary – contracting area, $A_1(\alpha)$ – Avrami (1st order), $A_2(\alpha)$ – Avrami (2nd order), $A_3(\alpha)$ – Avrami (3rd order).

Table 5 Frequency factors and activation energy for particle sizes of 5NU-h dehydration at 0% RH using $D_2(\alpha)$ as best fitting model

Particle size	Activation energy (kJ mol^{-1})	Frequency factor (s^{-1})	Linear regression (r^2)
425 μm	64	3.61×10^6	0.950
125 μm	124	2.36×10^{16}	0.926
100 μm	180	9.74×10^{24}	0.964

One striking result is that as the particle size is decreased, the activation energy of the dehydration process markedly increases (Table 5). A second unusual result is that the frequency factors generated for the smaller particle size fractions (125 μm and 100 μm) are in excess of those normally associated with crystalline lattices. This clearly shows that the crystallinity of these ground samples were affected, supporting the idea of amorphisation. Intuitively, it would be expected that smaller particles would have lower activation energies. But the combination of the increase in frequency factors and the knowledge that dehydration occurs though a major reorganization of the lattice indicates that this is likely to affect the activation energy. Grinding causes a phase change and water loss from the lattice, but the water is likely to be trapped both in the particulates and between them.

In the case of changes in relative humidity (Fig. 14), the dehydration curves are again stepwise. However, for these runs, the model that best fits is again the Valensi–Barrer equation. As the relative humidity increases, the rate of dehydration decreases (for this sample, as-grown crystals, Table 6). The lower the relative humidity, the more monotonic the dehydration curve. As expected (for this size of crystal), the activation energy for the dehydration process increased, but not as significantly as for the case of reduced particle size. The frequency factors calculated are within the range of those observed for crystalline lattices.

This supports the idea that as water is lost from 5NU-h, phase re-organisation at the surface means that there are times when the water cannot leave the crystal. As the temperature increases, the increased vapour pressure generated means that the curves take on a more classically observed sigmoidal shape. This brings up the question of how this data ought to be analysed. Returning to the ideas of how water is lost at the molecular level, the water loss is a combination of disassociation of water from the hydrate crystal and then its ability to permeate through the layer of anhydrous material blocking its exit path, either through the surface layer of dehydrated material, or *via* the cracks evolving parallel to the $(10\bar{2})$ planes. With this in mind, it is clear that none of the available kinetic models are directly of use.

Rehydration. 5NU will not undergo a rehydration when exposed to water vapour, unlike the case of oxalic acid. This is not entirely unexpected. It has already been shown that even in aqueous solutions, it can take up to 8 days for a solvent mediated phase transformation to occur, turning the anhydrous forms into the hydrated form.[7]

Conclusions

The dehydration process of the simple molecular solid 5NU, like the case of oxalic acid before, has been shown to be more complex than previously imagined. Microscopic observations show that in addition to the molecular disassociation between the 5NU and water molecules, recrystallisation and macroscopic structural developments (cracks *etc.*) also play a part in

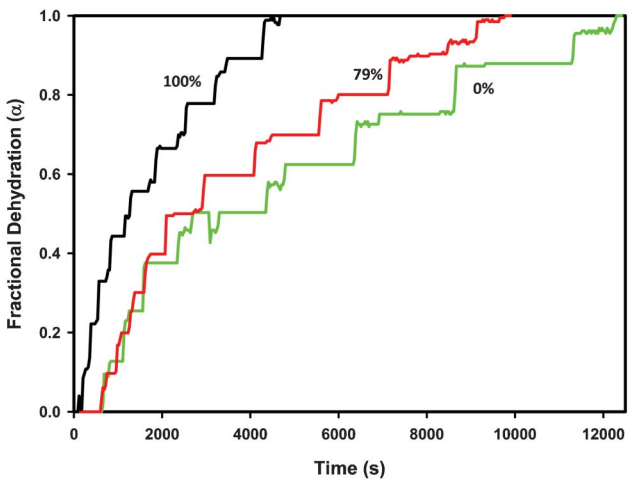

Fig. 14 Thermal dehydration with differing relative humidities.

Table 6 Frequency factors and activation energies for the dehydration of 'as crystallised' 5NU-h at differing relative humidities, using $D_2(\alpha)$ as best fitting model

Relative humidity	Activation energy (kJ mol^{-1})	Frequency factor (s^{-1})	Linear regression (r^2)
0%	83	5.42×10^9	0.990
79%	95	2.00×10^{11}	0.949
100%	115	2.42×10^{14}	0.951

the dehydration process. There are two areas that are still unclear from our study, firstly, does the dehydrated 5NU initially become an amorphous solid, prior to recrystallisation into 5NU-m? Secondly, given the stepwise nature of the weight loss during the dehydration process, what is happening during this hiatus? Does the water continue to disassociate from the 5NU-h crystal substructure, but is then trapped within the particle by the outer layers? Or does the trapped water generate a very localized high relative humidity, stopping the disassociation?

Clearly changing the physical properties of the crystalline hydrate does affect the physical characteristics. Grinding lessens the water content of the finer crystals and the frequency factors imply that there is an excess of non-crystalline material. However, as has been mentioned earlier, the nature of the derivation of these frequency factors means that they cannot be used without some regard to what is really happening.

The stepwise nature of the dehydration process as observed by thermogravimetric methods does mean that the standard kinetic models are definitely lacking. Although they have been used in this paper, to generate an ''average'' fit, none of them accurately describe the mechanistic processes occurring. Given that these appear not only for 5NU, but also as has been noted, at a lesser level for oxalic acid, much more thought and experimentation needs be directed to understanding this procedure.

Within the current thinking of dehydration, 5NU-h appears to be a channel hydrate, but clearly is not. It is chemically intuitive that most (if not all) bound hydrates will have apparent channels or directions of easy dehydration. Examination of any given hydrate is likely to yield a view where the water molecules line up in a particular direction. But the voids that may be left (as in this case) will no doubt be blocked by steric effects.

Within the Galwey WET characterization, the behaviour of 5NU does most readily fit into the WET 3 category. This categorises the reaction as an interfacial deceleratory reaction. However, as with oxalic acid, this does not quite cover the entire process seen. In the case of 5NU, microscopic observations show water extant at the crystal surface, which is not described within any categories of the WET classification. Nevertheless, it does point to 5NU-h being part of that grouping, although it is likely to be another WET 3 subset (of which Galwey describes four). However there can still be questions as to whether there are elements of WET 4 behaviour. In particular, the description of the pressure release of water at the surface is akin to a localized explosive disintegration at the surface (Galwey's Wet 4A). But it should not be forgotten that the Galwey classification system is based upon observations of dehydration in inorganic hydrates. So it ought not be too surprising that the WET classification system does not fully encompass the behaviour of organic hydrates, even for relatively conformationally inflexible ones such as 5NU.

The system of Petit and Coquerel gives a much clearer definition of the process. Their classification scheme can be followed using the flow chart given in their paper[5] and a copy of the scheme is given as electronic supplementary data (ESI†). The first choice is whether there exists ''channels or planes exclusively occupied by water molecules or possibility of cooperative structural deformation leading to these channels or planes''. The above work has shown that these channels do not exist (even though they appear to). This leads to the fact that there is a ''destructive dehydration departure of water molecules generates amorphous materials''. The choices from this decision block are simple, either 5NU remains amorphous, or it recrystallises. Again, we have shown that the resultant product is the 5NU-o phase and thus must recrystallise. This leads to the classification of the process as a Class I Destructive-Crystallised reaction (I-D.C.). There are still issues with this classification. There is no direct evidence of an intermediate amorphous phase, although the arguments given above imply that this is likely to be the case. We believe that this is just an experimental limitation of being able to study small amounts of amorphous organic phases, where signals are subsumed by those of the crystalline phase that surrounds it.

As with oxalic acid, the dehydration behaviour of as simple a system as 5NU-h is more complex than previously imagined. At the molecular level, the packing of the 5NU-h crystal points to how water can escape, but the interrelationship between 5NU-h and the resultant phase 5NU-o also means that these escape routes are easily blocked. The lattice mismatch and blocking of these escape routes means that larger scale damage must occur for any further water loss to take place. This is seen and accounts well for the stepwise weight loss observed.

The inability of current kinetic models to truly account for the observed data is likely to be the tip of the iceberg for closer examination of many organic hydrates. It must be held in mind that many (if not all) of these are based on the dehydration of inorganic hydrates, as is the majority of the Galwey classification, and even the original work by Petit and Coquerel. For organic molecules, dominated by hydrogen and van der Waals bonding and more so for larger ones with much

more structural flexibility, these classifications are an excellent start to understanding the dehydration process. But much more work needs be done to be able to expand them to cover the broader range of conformations and structures that molecular materials can have.

References

1 (*a*) J. Bernstein, in *Polymorphism in Molecular Crystals*, Oxford University Press, Oxford, UK, 1st edn, 2002; (*b*) J. Bernstein, *Cryst. Growth Des.*, 2011, **11**, 632–650.
2 (*a*) D. Zhou, E. A. Schmitt, G. G. Z. Zhang, D. Law, C. A. Wright, S. Vyazovkin and D. J. W. Grant, *J. Pharm. Sci.*, 2003, **92**, 1367–1376; (*b*) A. K. Sameleh and L. S. Taylor, *J. Pharm. Sci.*, 2006, **95**, 446–461; (*c*) M. M. Nolasco, A. M. Amado and P. J. A. Ribeiro-Claro, *J. Raman Spectrosc.*, 2010, **41**, 340–349.
3 (*a*) M. E. Brown, D. Dollimore and A. K. Galwey, in *Reactions in the Solid State*, Comprehensive Chemical Kinetics, Elsevier, Amsterdam, 1980, vol. 22; (*b*) A. K. Galwey and M. E. Brown, *Thermal Decomposition of Ionic Solids*, Elsevier, Amsterdam, 1999; (*c*) W. E. Garner, in *Chemistry of the Solid-State*, ed. W. E. Garner, Butterworth, London, 1955, p. 213; (*d*) P. W. Jacobs and F. C. Tompkins, in *Chemistry of the Solid-State*, ed. W. E. Garner, Butterworth, London, 1955, ch. 7.
4 M. O. Okoth, R. M. Vrcelj, D. B. Sheen and J. N. Sherwood, *CrystEngComm*, 2012, **14**, 1602–1612.
5 (*a*) A. K. Galwey, *Thermochim. Acta*, 2000, **355**, 181–238; (*b*) S. Petit and G. Coquerel, *Chem. Mater.*, 1996, **8**, 2247–2258; (*c*) P. R. Perrier and R. S. Byrn, *J. Org. Chem.*, 1982, **47**, 4671–4676.
6 (*a*) B. M. Craven, *Acta Crystallogr.*, 1967, **23**, 376–383; (*b*) B. M. Pierce and R. M. Wing, *Proc. SPIE Inti. Soc. Opt. Eng.*, 1987, **682**, 27–35; (*c*) A. R. Kennedy, M. O. Okoth, D. B. Sheen, J. N. Sherwood and R. M. Vrcelj, *Acta Crystallogr.*, 1998, **C54**, 547–550; (*d*) R. S. Gopalan, U. K. Giridhar and C. N. R. Rao, *ChemPhysChem*, 2000, **1**, 127–135; (*e*) P. S. Pereira Silva, S. R. Domingos, M. Ramos Silva, J. A. Paixão and A. Matos Beja, *Acta Crystallogr.*, 2008, **E64**, o1091; (*f*) P. S. Pereira Silva, personal communication, 2011.
7 M. O. Okoth, R. M. Vrcelj, M. B. Pitak, D. B. Sheen and J. N. Sherwood, *Cryst. Growth Des.*, 2012, **12**, 5002–5011.
8 C. O. Agbada, Ph.D. Thesis, University of Bradford, 1991.
9 M. U. A. Ahlqvist and L. S. Taylor, *Int. J. Pharm.*, 2002, **241**, 253–261.
10 (*a*) H. Tanaka and N. Koga, *J. Phys. Chem.*, 1988, **92**, 7023–7029; (*b*) A. K. Galwey, N. Koga and H. Tanaka, *J. Chem. Soc., Faraday Trans.*, 1990, **86**, 531–537.
11 T. Ozawa, *J. Thermal Anal.*, 1970, **2**, 301–324.
12 M. O. Okoth, Ph.D. Thesis, University of Strathclyde, 2002.